

## TOWARDS THE IMPROVEMENT OF THE STABILITY OF A-SI:H PIN DEVICES

**R. Martins, H. Águas, I. Ferreira, E. Fortunato and L. Guimarães**

CENIMAT, DCM da Faculdade de Ciências e Tecnologia da Universidade Nova de Lisboa and CEMOP-UNINOVA, Quinta da Torre, 2825-114 Monte de Caparica (Portugal)

**Abstract** - This paper deals with a new process aiming to improve the stability of a-Si:H pin solar cells deposited on a single batch process, by proper passivation of the interfaces. The process consists in partially removing a deposited sacrificial oxide layer grown between the p/i and/or i/n interfaces by proper SF<sub>6</sub> etching. This layer is an absorber of defects and impurities that are introduced in the interfaces, mainly from the chamber walls and the substrate surface. The results achieved in laboratory samples lead to devices in which the fill factor and short circuit current density were improved respectively towards 75% and 16.5 mAcm<sup>-2</sup>, with a final working efficiency of about 9.5%.

### 1. INTRODUCTION

One of the main problems of the a-Si:H pin solar cell devices concerns their stability due to light soaking effect (Schropp et al., 1998) that degrades the device performances. The induced light defects are usually attributed to malfunctions of the device interfaces (Catalano et al., 1991 and Fantoni et al., 1999). To overcome this problem several methods have been proposed such as the use of blocking layers, grading or p<sup>+</sup> multi-layered, i/n interface grading, tailoring of the i layer (Schropp et al., 1995), together with the use of multichamber systems (Maruyama et al., 1995) or by producing tandem type solar cells (Guha 1999). In spite of all these the stability of the a-Si:H solar cells still remain to be solved. Apart from that, the cross contamination of devices produced in a single chamber system also limits their performances (Maruyama et al., 1995).

In this paper we propose a process aiming to improve the performances and stability of devices produced in single chamber systems. It consists in growing at the interfaces an oxide based interlayer (s) produced by PECVD technique, followed by its controlled ablation. This allows producing grading and smoothing interfaces where most of adsorbed defects and impurities that tend to build up at the interfaces are removed. That is, the interlayer promotes the interface densification and compensates any possible electric field distortion in the interface. This leads to the increase of the solar cell stability from about 75% to about 90% and to increase their running efficiencies ( $\eta$ ) from about 7% to about 9.5%.

### 2. EXPERIMENTAL DETAILS

The pin solar cells were deposited in a conventional single chamber r.f. Plasma Enhanced Chemical Vapour Deposition-PECVD system, able to handle twelve 10cm×10cm substrates, under low self and substrate ion bombardment conditions, close to the edge of the powder formation regime (Martins et al., 1999).

The substrates were SnO<sub>2</sub> coated glass, with a smooth surface and a sheet resistance < 20  $\square$ /sq. To deposit n

undoped (i) and p-doped films, mixed bottle of PH<sub>3</sub> (0.7%)+SiH<sub>4</sub> (15.1%)+H<sub>2</sub> (2%)+He (82.2%), pure SiH<sub>4</sub> and a mixture of B<sub>2</sub>H<sub>6</sub> (0.2%) + SiH<sub>4</sub> (44.2%) + CH<sub>4</sub> (33.4%) + H<sub>2</sub> (22.2%) were used. The gas flows ranged from 1 sccm to 50 sccm and the power densities ranged from 15 mWcm<sup>-2</sup> to 100 mWcm<sup>-2</sup>, selected for each case to keep the plasma resistance only slightly larger than the plasma reactance (Martins et al., 1999). The substrate temperatures were around 480 °K while the pressure was 80 Pa for all sets of films produced. The main properties of the layers used are listed in table 1.

**Table 1.** Main electrical and optical properties of the p, i and n a-Si:H layers used.

Properties	p layer	i layer	n layer
$\sigma_d$ Scm <sup>-1</sup>	6×10 <sup>-6</sup>	5×10 <sup>-11</sup>	4.5×10 <sup>-2</sup>
$\Delta E$ (eV)	0.19	0.84	0.10
$E_{op}$ (eV)	1.82	1.63	1.78
$\sigma_{ph}$ Scm <sup>-1</sup>	---	4×10 <sup>-5</sup>	---

The s-layer was produced by blowing oxygen (O<sub>2</sub>) to the p (or i) followed by an O<sub>2</sub> plasma (Fortunato et al., 1998 and Ponpon et al., 1982) and the growth of a <1 nm intrinsic layer. The plasma oxidation had a duration of 5 minutes. The oxidation conditions were substrate temperature of 570 °C, O<sub>2</sub> pressure of 20 Pa (150 mTorr) and rf power of 60 W. After each oxidation step the thickness was measured in a dummy sample by spectroscopic ellipsometry between 1.5 and 5 eV using a Jobin Yvon H10 ellipsometer. After that, the oxide was characterised by Fourier Transformed Infrared Spectroscopy (Queeney et al., 2000) in a ATI Mattson Genesis series, using as reference a double face polished undoped crystalline silicon sample.

The thicknesses of the oxides were measured on a dummy sample by spectroscopic ellipsometry. To determine the oxide thickness we use a simple model that consists on a SiO<sub>2</sub> layer over a c-Si substrate. The optical constants of the materials were taken from the database that comes with the DelPsi software of Jobin Yvon and correspond to pure SiO<sub>2</sub> and pure c-Si.

The s-layer behaves as an absorber of boron atoms, similarly what happens in oxide layer grown on the top of

crystalline silicon p-type film (Grove 1967), leading to a substantial decrease of its concentration in the p-layer, close to the s-layer. Therefore, grading boron like profile is expected along the p-layer thickness.

The partial ablation of this s-layer were made either using a SF<sub>6</sub> plasma (s<sub>p</sub>) or by flushing SF<sub>6</sub> into the reactor (s<sub>b</sub>) for 2 minutes. A hydrogen (H<sub>2</sub>) flush and discharge, with an estimated etching rate of about 0.01 nm/s always followed the SF<sub>6</sub> process, in order to eliminate possible Sulphurous traces left by the SF<sub>6</sub> plasma discharge. The SF<sub>6</sub> gas flow used was of about 40 sccm, the pressure was kept at about 13 Pa and the power used was of about 60 W. This procedure leads to the production of grading and smooth interfaces, decreases the impurity cross contamination and the remaining s<sub>(b/p)</sub> layer prevents the recombination of the photogenerated electrons and their positive counterparts. That is, it passivates the interface, compensating also possible defects.

In this study the reactor was properly cleaned followed by the deposition of an i-layer to render passive the entire chamber in-walls. The thickness (d) of the different layers were previously determined using a Sloan Dektak profilometer. This allows determining the growth and the etching rates of the different layers and so, to establish the d of the different layers of the device, including the etching procedures.

The thickness of the p and n layers were fixed at 16 nm and 40 nm, respectively, while the thickness of the i-varied aiming to determine the d that produces devices with the largest efficiencies ( $\eta$ ). The back metal contact of the devices studied was Al deposited by thermal evaporation and the devices were cured at 420 °K for 1 h, in a forming gas atmosphere.

The current density as a function of voltage J(V) curves and the degradation data as a function of the time were taken under Air Mass 1.5 (AM1.5) global solar spectrum conditions (100 mWcm<sup>-2</sup>), using a calibrated a-Si:H solar cell as reference and controlled by a dedicated computer control system. The dimensions of the cells tests were about 25 mm<sup>2</sup>, spread over the entire 10 cm×10 cm substrate, aiming to determine the reliability of the process when large area cells are needed to be produced.

### 3. RESULTS

#### 3.1 Oxide film

Figure 1 shows the infrared stretching peak associated with the Si-O groups for the oxides produced. There we notice that the peaks are centred at about 1050 cm<sup>-1</sup>.

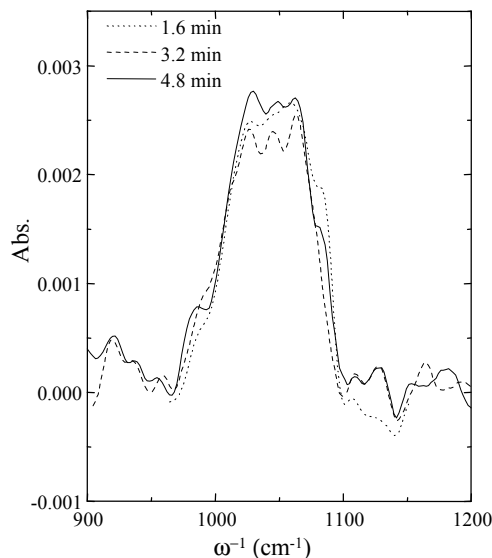


Figure 1. Evolution of the Si-O stretching mode after oxygen plasma oxidation, for different process times as labelled in the figure.

This peak can be attributed to a compact oxide promoted by the O<sup>+</sup> bombardment from the plasma. This bombardment could also lead to a micro-etching of the surface and to a red shift in the Si-O stretching mode due to a slightly increase of the compressive stress in the Si/SiO<sub>2</sub> interface (Charvet et al., 1999, Águas et al., 2000 and Oehrlein 1997). Another effect that can be associated with a reduction in the high energy component of the stretching peak is the reduction of the interface roughness as was found in the simulation studies using the EMA (effective medium approximation) performed by Queeney and co workers (Charvet et al., 1999). This means that the O<sup>+</sup> bombardment from the plasma can assist the formation of a uniform interface and so to passivate their defects.

In figure 2 we depict the behaviour of the oxide thickness with the oxide time. Apart from that, we also show the dependence of the  $\chi^2$  value that represents the relative error between the refractive index of the model used to fit the oxide thickness and the experimental measure. This means that as the  $\chi^2$  value becomes closer to zero, the optical properties of the grown oxide became closer to the SiO<sub>2</sub> properties used as a reference in the model and so, a better quality for the oxide grown.

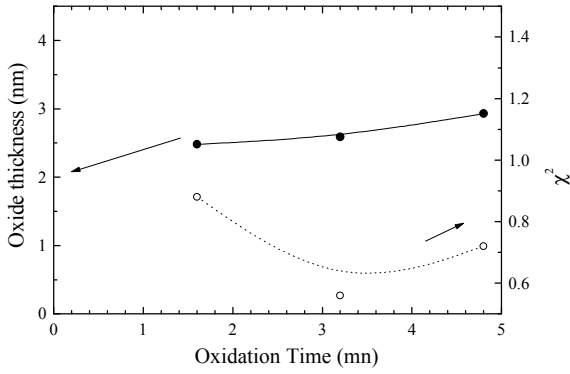


Figure 2- Dependence of the oxide thickness and  $\chi^2$  on the oxidation time.

The data achieved show that the best oxide layer is produced by using an oxide time of about 3 min. This was the condition used to grow the oxide interlayer used during the production of the different types of solar cells.

### 3.2 Device Behaviour

Figure 3 shows the dependence of the open circuit voltage ( $V_{oc}$ ), fill factor (FF), short circuit current density ( $J_{sc}$ ) and  $\eta$  on  $d$  of the i-layer of devices produced without applying the proposed method (type A cells).

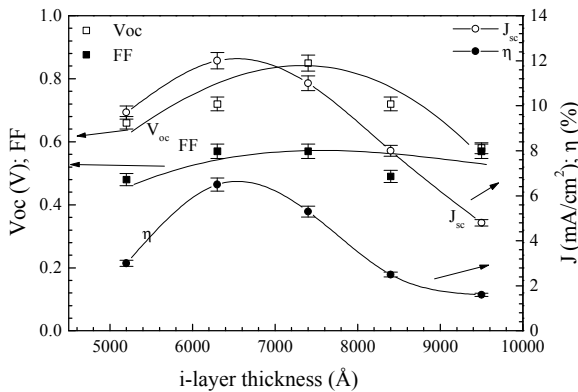


Figure 3. Dependence of  $V_{oc}$ , FF,  $J_{sc}$  and  $\eta$  on  $d$  of the i-layer, in type A cells. The lines are to guide the eyes.

Here, the thickness of the p and n layers were fixed respectively equal to 16 nm and 40 nm. From this result we fix for the i-layer the value of 640 nm, the one that had the largest  $\eta$ .

After that, three different types of cells were grown. Device B was produced using a  $s_p$  interlayer located at the p/i interface [p/ $s_p$ /i/n]. Device C was produced using a  $s_b$  interlayer at the p/i interface [p/ $s_b$ /i/n]. Device D was produced using the  $s_b$  interlayers in both p/i and i/n interfaces [p/ $s_b$ /i/ $s_b$ /n]. The main performances of the set of solar cells analysed before degradation experiments are shown in table 2. All data were taken with an AM1.5 global, 100 mWcm<sup>-2</sup> solar spectrum. Here we have to mention that the results depicted in table 2 refer to the average values achieved along different trials.

**Table 2** Structure and properties of the cells studied before degradation experiments.

Details	A	B	C	D
Structure Ref. cell	p/ $s_p$ /i/n	p/ $s_b$ /i/n	p/ $s_b$ /i/n	p/ $s_b$ /i/ $s_b$ /n
$J_{sc}$ (mA)	14.10 $\pm 0.43$	8.0 $\pm 0.24$	16.20 $\pm 0.49$	15.00 $\pm 0.45$
$V_{oc}$ (V)	0.80 $\pm 0.02$	0.75 $\pm 0.02$	0.81 $\pm 0.02$	0.91 $\pm 0.03$
FF (%)	62 $\pm 2.1$	42 $\pm 1.5$	73 $\pm 2.6$	58 $\pm 2$
$\eta$ (%)	7.00 $\pm 0.28$	2.42 $\pm 0.10$	9.86 $\pm 0.40$	8.13 $\pm 0.33$

The light soaking experiments performed showed that device A experienced a light degradation of about 25% after being exposed to 250 AM1.5 light hours while the degradation observed in devices C, D and B was respectively of about 8%, 10% and 15%, as can be seen in figure 4.

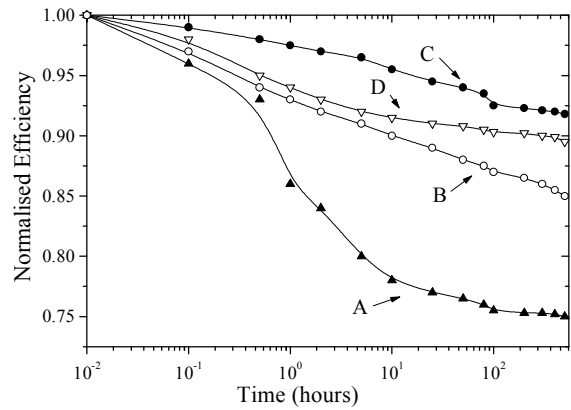


Figure 4. Relative changes of the normalised  $\eta$  of the devices studied during continuous light soaking experiment with an AM 1.5 global spectrum. The lines are to guide the eyes.

## 4. ANALYSIS AND DISCUSSION

The set of results achieved show that oxide films with the required stoichiometry and compactness can be grown by PECVD. There, we also notice that the  $O^+$  bombardment sustained by the growth surface lead to the improvement of the quality of the oxide layer grown.

As far as the devices grown are concerned, the data depicted in figure 3 clear show that the i-layer thickness plays an important role in determining the final device performances.

The limitations observed in the performances of device A ( $\eta \leq 7\%$ , with  $FF \leq 63\%$ ) are attributed to the fact of using a single chamber to process all layers (Schmitt et al., 1988).

The data of curve B indicate that the use of a SF<sub>6</sub> plasma degrades the main device parameters (J<sub>sc</sub>, FF and V<sub>oc</sub> are reduced, respectively, by more than 45 %, 33% and 6.5%), leading to a η reduction of about 65% (see table 2). This reduction is attributed to sulphurs contamination of the reactor that is retained within the chamber even after the H<sub>2</sub> flush and discharge.

The performances of devices C and D shown in table 2 reveal that the method applied to passivate the p/i and i/n interfaces lead to an overall improvement of their characteristics. The data of device C show that J<sub>sc</sub>, FF and η are respectively increased by 15%, 19% and 39%, while V<sub>oc</sub> remains almost the same. This result means that ablation process was successfully achieved and that SF<sub>6</sub> should react spontaneously with all deposited layers containing boron doped atoms, leading to an overall improvement of the device, similarly to what was observed with NF<sub>3</sub> (Catalano et al., 1988).

For device D the data show that J<sub>sc</sub> increased about 6%, FF decreased about 6% and V<sub>oc</sub> increased about 16%, corresponding to an overall increase of η of about 15% in relation to cell A.

The decrease of J<sub>sc</sub> and the increase of V<sub>oc</sub> in device D is attributed to the effect of the interlayer (s<sub>b</sub>) in the i/n interface. Here, the data indicate that the expected spontaneous reaction of SF<sub>6</sub> with the i-layer did not occur and so, a less effective ablation of the interlayer was achieved. Thus, V<sub>oc</sub> increased due to the presence of an effective barrier that seems to prevent the access of carriers to the interfacial defects (Schropp et al., 1995) while J<sub>sc</sub> decreased, due to the barrier thickness or improper graded process (Guha 1999). These parameters increase carrier losses and so, reduced the shunt resistance, explaining the FF obtained. In spite of this, η is larger than that of cell A (about 15%).

The behaviours observed in the different cells were obtained in more than 90% of the devices build in the substrate area of 10 cm×10 cm.

The light soaking results are shown in figure 4. Here, we must emphasise that most of the degradation behaviour observed is due to a faster degradation of FF, since V<sub>oc</sub> remains almost constant and J<sub>sc</sub> is little affected by the light soaking experiments. The data show that the method proposed to passivate the interfaces leads to more stable devices, especially when applied to the p/i interface (cell C). The lower stability detected in sample D is attributed to a deleterious effect of the interlayer located at the i/n interface, due to the failure of the SF<sub>6</sub> flush to partially remove it, similarly as it happens with the p/i interface. On the other hand, the poor performances of device B are attributed to the S contamination of the chamber, together with an erratic ablation of the interlayer, under SF<sub>6</sub> plasma conditions.

## 5. CONCLUSIONS

We have successfully fabricated stable pin devices with efficiencies of about 9% by proper design of the p/i

interface. The results achieved lead to an increase of the device efficiency by more than 30%, when compared with conventional solar cells. Besides that, the stability is increased by about a factor of 4, when compared with conventional devices produced in the same chamber reactor.

Apart from that, the results obtained show that the interlayer placed in the i/n interface does not work so effectively as expected. Thus, future work will be placed aiming to improve this interface and so, the set of device performances achieved until now, prior to transfer then to an inline multiple chamber system.

## ACKNOWLEDGMENTS

The authors would like to thank to N. Martins and J. Ferreira for the help given in the sample preparation to perform the conductivity measurements. We also thank the “Fundação para a Ciência e Tecnologia” for the support given through “Financiamentos Plurianuais CENIMAT” and projects PRAXIS/3/3.1/MMA/1788/95 and PRAXIS/P/CTM/12094/1998. Apart from that, thanks are due to the project H-Alpha Solar, under contract n° ERK6-CT-1999-00004 and to “Fundação Gulbenkian” for the support given to one of the authors to attend the Eurosun 2000 Conference.

## REFERENCES

- Schropp R.E.I. and Zeman M. (1998) *Amorphous and Microcrystalline Silicon Solar Cells*, pp. 69-109. Kluwer Academic Publishers, London.
- Catalano A. (1991) *In Amorphous and Microcrystalline Semiconductor Devices: Optoelectronic Devices*, J. Kanicki (Ed.), Vol. 1, pp. 9-73. Artech House Inc., Norwood, MA, U.S.A.
- Fantoni A., Vieira M., Martins R. (1999). *Simulation of Hydrogenated amorphous and microcrystalline Silicon optoelectronic devices*. J. Mathematics and Computers Simulation 49, 381-401.
- Schropp R.E.I. (1995). *In Hydrogenated Amorphous Silicon*. H. Neber-Aeschbacher (Ed.), Vol. 44-46, pp. 853-861, Part 2. Scitec Publications, Zurich.
- Maruyama E., Tsuda S., Nakano S. (1995) *In Hydrogenated Amorphous Silicon*. H. Neber-Aeschbacher (Ed.), Vol. 44-46, pp. 863-879, Part 2. Scitec Publications, Zurich.
- Guha S. (1999). *In Technology and Applications of Amorphous Silicon*, Street R. (Ed.), Vol. 37, pp. 255-305. Springer-Verlag, Berlin.
- Martins R., Silva V., Ferreira I., Domingues A. and Fortunato E. (1999). Role of the gas temperature and power to gas flow ratio on powder formation in films grown by PECVD technique. *Vacuum* 56, 25-30.

Fortunato E., Malik A., Martins R. (1998). Thin Oxide Interface Layers in a-Si:H MIS Structures. *J. Non-Crystalline Solids* 227-230, 1230-1234.

Ponpon J.P. and Bourdon B. (1982). Oxidation of glow discharge a-Si:H. *Solid State Electronics* 25, 875-876.

Queeney K., Weldon M., Chang J., Chabal Y., Gurevich A., Sapjeta J. and Opila R. (2000). Infrared spectroscopic analysis of Si/SiO<sub>2</sub> interface structure of thermally oxidized silicon. *J. Appl. Phys.*, 87 1322-1330.

Grove S. (1967). *Physics and Technology of Semiconductor Devices*. Wiley, N.Y.

Charvet S., Madelon R., Gourbilleau F. and Rizk R. (1999). Spectroscopic ellipsometry analyses of sputtered Si/SiO<sub>2</sub> nanostructures. *J. Appl. Phys.*, 85, 4032-4039.

Águas H., Martins R., Ferreira I. and Fortunato E. Correlation between surface/interface states and the performances of MIS structures. *In Proceedings of Symp. A, MRS Spring Meeting*, S. Francisco, USA, 20-25 April. In Press.

Oehrlein G.S. (1997). *In Plasma Processing of Semiconductors*, Applied Science Series, **336**, ed. by P.F. Williams, pp. 73-88. NATO series Boston.

Schmitt J.P.M., Meot J., Roubeau P., Parrens P. (1988). New reactor design for low contamination amorphous silicon deposition. *In Proceedings of 8<sup>th</sup> Europ. Comm. Photov. Solar En. Conf.*, Florence, Italy, Solomon I., Equer B. and Helm P. (Eds), pp 964-968, Kluwer Academic Publishers, London.

Catalano A., Wood G. (1988). Short wavelength response in a-Si:H p-i-n diodes: a simple method to minimise interface recombination, *J. Appl. Phys.*, 63, 1220-1223.

